THE AMERICAN SOCIETY OF MECHANICAL ENGINEERS
345 E. 47th St., New York, N.Y. 10017

97-AA-113

Analysis of Windmilling Characteristics for a Twin-Spool Turbofan Engine

by

Min-Su Choi†, In-Shik Kang††, Jin-Shik Lim†, and Yong-Shik Hong†††

Abstract

The windmilling characteristics of twin-spool, high bypass ratio turbofan engine have been analyzed. This analysis is an extension of the previously reported analysis for a single-spool turbojet engine. As before, the aerodynamic performances of engine components are determined by incorporating the available cascade loss correlations. For a given flight condition, the steady-state windmilling conditions are determined by iteratively balancing the mass flow rate and angular momentum through the two spools. Compared to the turbojet analysis, the new analysis requires determination of bypass ratio and work split between the two spools. Some of the calculation results have been compared against the limited data available for a CF-6 engine, and the two show good agreement. The present method is thus shown to be capable in predicting turbofan engine's windmilling characteristics during its design stage.

Nomenclature

$\dot{m}_a$	engine air flow rate
$\dot{m}_{bypass}$	bypass air flow rate
$\dot{m}_{core}$	core air flow rate
A	intake area
AR	aspect ratio of blade
b	coefficient in the C_{Dp} eq.
C_{Da}	annulus wall drag coefficient
C_{Dp}	profile drag coefficient
C_{Ds}	secondary loss drag coefficient
C_L	lift coefficient
h	altitude
H	blade height
HP	high pressure spool
HPC	high pressure compressor
HPT	high pressure turbine
LP	low pressure spool
LPC	low pressure compressor
LPT	low pressure turbine
N	rotational rpm
t	tip clearance
T_q	torque
V	flight speed
η_{loss}	efficiency loss
ρ	air density

Subscript

a	ambient condition
f	friction
l	accessary driven load
T	total or stagnation

1. Introduction

Windmilling of a gas turbine engine during flight occurs after the engine flame-out. So understanding of windmilling characteristics of gas turbine engines is required for the design of an engine restart system. Generally, the civil turbofan engines can be restarted in flight if its rotational speed obtained by windmilling is greater than approximately 10% of its maximum operational speed[1].

In the previous analysis[2], the computed results of single-spool turbojet engine's windmilling performance calculation results showed good agreement with the experimental data. The inlet flow condition during windmilling of a single-spool engine remains

† Agency for Defense Development, Taejon, 305-600, KOREA.
†† Hyundai Space & Aircraft Co., LTD. Kyungki-Do, 449-910, KOREA.
††† Professor, Department of Aerospace Engineering, INHA University, Inchon, 402-751, KOREA.

Presented at the ASME ASIA '97 Congress & Exhibition
Singapore – September 30–October 2, 1997

constant until the engine reaches a certain speed, because it has one flow path and one exhaust nozzle. It means that the windmilling prediction algorithm is stable and rapid.

However, the algorithm for twin-spool turbofan engines is more complex, because the matching process of each spool should be coupled to each other in view of air flow rate.

Shou[3] developed three theoretical methods for predicting the windmilling characteristics of several single-spool turbojet engines. Morita and Sasaki[4] analyzed the in flight starting process of turbofan engines using actual experimental data. But their method can not be applied to different type engines because it is based on experimental data of a specific engine.

The objective of the present work is to develop a method to predict twin-spool turbofan engine's windmilling characteristics which can be used in the preliminary design stages of engine development.

2. Calculation Procedure

The numerical calculation procedure is mainly composed of dual iteration loops as shown in Fig. 1. Two inner loops determine the windmilling operation conditions of each component by satisfying matching continuity in LP and HP spools. At each iteration step, the torques of rotating components are calculated. However, the final operation condition is established through the outer loop calculation in which the excess torques of LPT and HPT are calculated, because there remains the torque imbalance between compressor and turbine in each spool.

3. Air Flow Rate Determination Through Inner Loops

Turbofan engine's exhaust system is composed of the main nozzle and the bypass nozzle as shown in Fig. 2. During windmilling, the momentum comes from ram air coming to an engine. And the LP spool is only aerodynamically coupled to the HP spool.

An initial mass flow of the engine is assumed for calculation from Eq. (1).

$$\dot{m}_a = (\rho \cdot V \cdot A)_{inlet} \tag{1}$$

The air flow going through the fan is saperated by the island(Fig. 3). Hence, the core and bypass air flow rates should be calculated through separate loops.

In the first loop, the bypass nozzle's air flow rate is calculated using the estimated flow conditions at the fan outlet. Then, this estimate is compared with the guessed value until the air flow through the bypass nozzle becomes equal to that at bypass duct inlet.

In the second loop the air flow through the core spool can be also calculated in the same manner. The engine core air flow is initially assumed as the difference between the total engine air flow and the bypass flow. After calculating the losses through the booster, compressor, turbine and other components, the air flow through the main nozzle is obtained. If the core flow does not match the assumed value, then the bypass flow is calculated again by assuming a new value of the engine total air flow.

So the engine air flow condition is obtained by dual iterations of two inner loops as shown in Fig. 1.

4. Torque Calculation Through Outer Loop

The torques of compressors and turbines are calculated from their velocity diagrams, and each spool's rotational acceleration is determined from the torque difference between the two components.

When the rotational speed saturates, the sum of aerodynamic torques of rotating components becomes equal to the torque of mechanical friction. So, the excess torques of each spool are expressed as followings[5, 6].

$$\sum T_{q\,HP} = T_{q\,HPT} - T_{q\,HPC} - T_{q\,f} - T_{q\,l} \tag{2}$$

$$\sum T_{q\,LP} = T_{q\,LPT} - T_{q\,fan} - T_{q\,f} \tag{3}$$

Hence, the steady-state condition is found by the outer loop in Fig. 1.

5. Loss Through Axial Fan

The total pressure loss through the axial fan blade row comes from four different sources ; profile loss, annulus loss, secondary loss and tip clearance loss.

The profile drag coefficient, C_{Dp}, is expressed by Howell's correlation [7] for various incidence angles. The secondary flow loss coefficient, C_{Ds}, is estimated using Eq. (4) as suggested by Griepentrog [8]. The coefficient b can be assumed to be 0.018 because the Reynold's number during windmilling is very low according to Griepentrog [8].

$$C_{Ds} = b \cdot C_L^2 \tag{4}$$

Tip clearance in the fan stage causes efficiency loss. The efficiency loss, or total pressure loss, can be estimated from Fig.(3) for various tip clearance fractions. And the efficiency drop η_{loss} can be calculated by Eq.(5) [7].

$$\eta_{loss} = 2(t/H - 0.01) \tag{5}$$

The mean work done factor is also applied to account for the performance deterioration in multi-stage fan and compressor[7, 8, 9].

6. Other Losses

The aerodynamic performances of compressor and turbine are determined by using the same correlations used in the turbojet analysis [2]. The adiabatic efficiencies of air intake and nozzles are also assumed to be constant as before [2].

The total pressure loss in the combustion chamber is obtained from Fig. 5 for various flight Mach numbers [10].

The mechanical efficiency is assumed to be constant, and the power consumption of the alternator and other accessories driven by the HP spool is assumed to be proportional to the square of engine's rotational speed [11].

7. Comparison of the Prediction with Experimental Data

The windmilling predictions for a CF-6 engine were compared with its limited windmilling test data.[12] Fig. 6 shows that the predicted air flow rate against flight Mach number and altitude agree well to the test data in the lower Mach number flight region. The discrepancy in the higher Mach number region is likely caused by neglecting the compressibility effect in loss correlations.

Fig. 7 shows the predicted LP spool's windmilling speed against flight Mach number and altitude compared with the experimental data. LP spool's windmilling speed monotonically increases, like the air flow rate, when the flight speed increases.

The predicted windmilling speed and air flow rate of the HP spool is presented in Fig. 8 & 9. The windmilling test data of CF-6 engine's HP spool were not available at the time of this analysis. However, from the agreement shown in Fig. 6 and 7 between the predictions and the test data, the trends shown in Fig. 8 & 9 are probably accurate and they agree with the experimental data from other studies [4].

8. Sensitivity Analysis

A parametric study was carried out to examine the sensitivity of the above predictions on various engine geometric parameters. Table 1 shows how much a 1% variation of some geometric parameters of CF-6 twin-spool turbofan engine(e. g. fan deflection angle, nozzle area and turbine deflection angle) changes the engine windmilling characteristics. Cascade geometries at the mid-span were derived both from available information and through preliminary design approach using basic specifications of CF-6 engine [12].

Through this analysis, it is found that the engine windmilling characteristics is not so sensitive to the variation of fan blade deflection angle and LP turbine blade deflection angle. However, the variations in the bypass nozzle area and HPT blade deflection angle significantly influence the windmilling characteristics. Therefore, the designer who intends to improve the windmilling capability of an engine has to be selective in setting the values for the bypass nozzle area and HPT blade deflection angle.

9. Conclusion

Windmilling characteristics of a high-bypass, twin-spool, separate-nozzle turbofan engine has been analyzed by a practical prediction algorithm in which the available loss correlations are used in determining the losses of each major component.

A comparison of the predicted results with the available CF-6 turbofan engine's test data has shown to be in good agreement.

Present method does not require any experimental data for a specific engine but only requires basic geometric data. Also, the present method is sufficiently flexible to accomodate incorporation of different loss models. Thus, this method can be conveniently used in the early stages of twin-spool turbofan engine development.

References

(1) Airbus industrie, "A300 Flight Manual", Nov., 1982.

(2) M. S. Choi, J. S. Lim, Y. S. Hong, "A Practical Method for Predicting the Windmilling Characteristics of Simple Turbojet Engines", ASME Turbo ASIA 96, Jakarta Indonesia, 96-TA-60, Nov. 1996.

(3) Zhao Qi Shou, "Calculation of Windmilling Characteristics of Turbojet Engines", ASME Journal of Engineering for Power, Vol. 103, Jan., 1981, pp. 1-12.

(4) Mitsuo Morita, and Makoto Sasaki, "Restart Characteristics of Turbofan Engines", ISABE 89-7127, 9th, 1989, pp. 1200-1206.

(5) Cohen, H., Rogers G.F.C., and Saravanamutto, H.I.H., "Gas Turbine Theory", Longman, 1972.

(6) Agrawal, R. K., and Yunis, M., "A Generalized Mathematical Model to Estimate Gas Turbine Starting Characteristics", ASME Journal of Engineering for Power, Vol. 104, Jan., 1982, pp. 194-199.

(7) Horlock, J. H., "Axial Flow Compressors", Robert E.

Table 1. Results of parametric sensitivity analysis(CF-6, sea level, International Standard Atmosphere, Ma=0.8)

Windmilling performance parameters / Geometric parameters	LP spool RPM	LP spool mass flow rate	Pressure ratio at fan booster stage	HPC pressure ratio	LPT pressure ratio
Fan balde deflection angle	-	-	± 0.14 %	-	-
Bypass nozzle area	±0.37 %	±0.90 %	±0.98 %	-	-
HPT blade deflection angle	∓0.27 %	∓0.70 %	-	±0.13 %	±0.19 %
LPT blade deflection angle	-	-	±0.06 %	-	-

Krieger Pub. Co., 1973, pp. 55-60.

(8) Wallis, R. A., "Axial Flow Fans and Ducts", John Wiley & Sons. Inc., 1983.

(9) Hong, Y. S., "Gas Turbine Engines (in Korean)", Cheongmungak Press, Korea, 1983.

(10) Marek Dzida, and Krzysztof Losowski, "Experimental Investigation of Pressure Drop in the Combustion Chamber of Gas Turbine", ASME Paper No. 89-GT-247, June, 1989, pp.1-4.

(11) Rodgers, C., "Starting Torque Characteristics of Small Aircraft Gas Turbines and APU's", ASME Journal of Engineering for Power, Vol. 102, Apr., 1980, pp. 231-238.

(12) General Electric, "CF6 Engine Facilities Planning Manual", Aug., 1976.

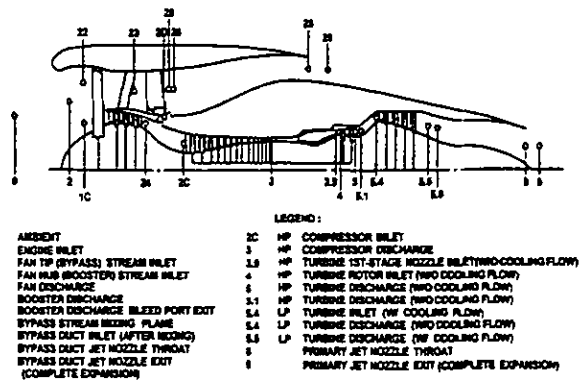

Fig. 2 Schematic diagram of CF-6 engine

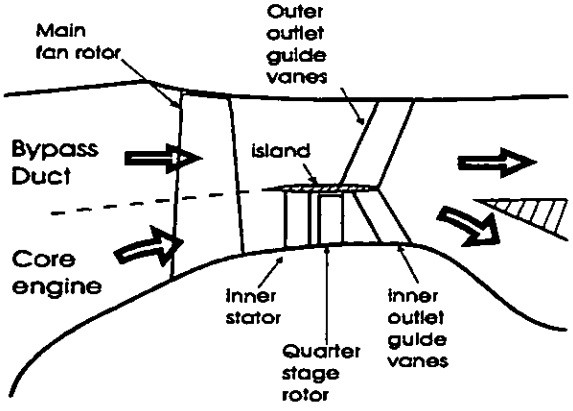

Fig. 3 The fan and booster stage of a high bypass-ratio turbofan engine.

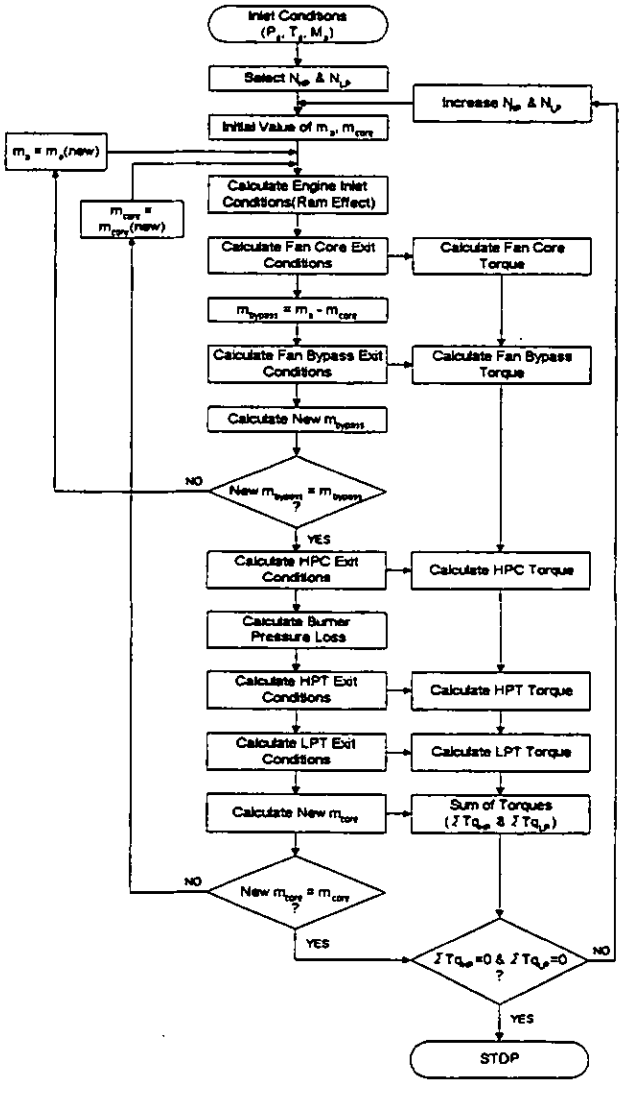

Fig. 1 Calculation process

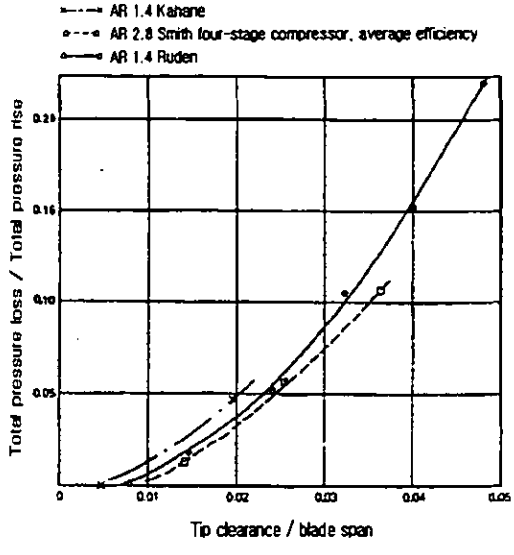

Fig. 4 Pressure loss factor versus tip clearance ratio[7]

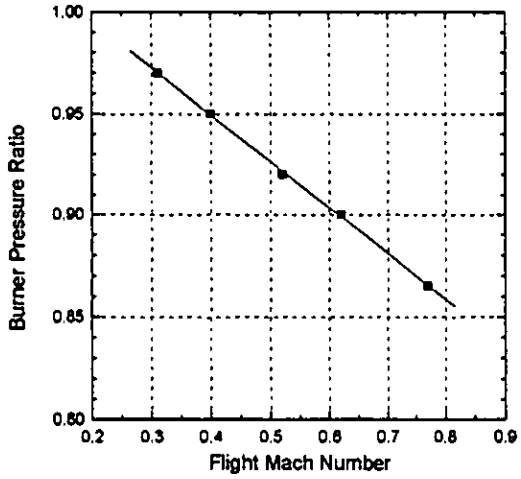

Fig. 5 Burner pressure ratio[3, 10]

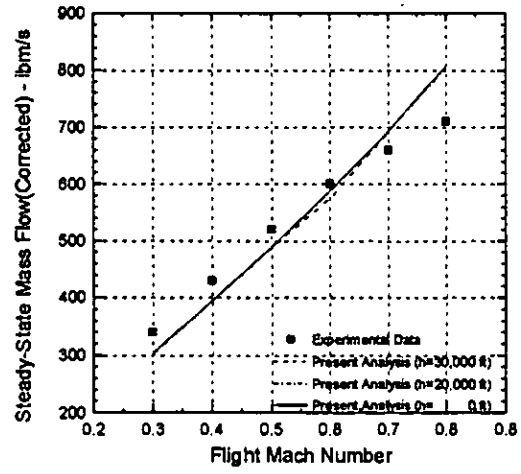

Fig. 6 Steady-state windmilling air flow rate of LP spool

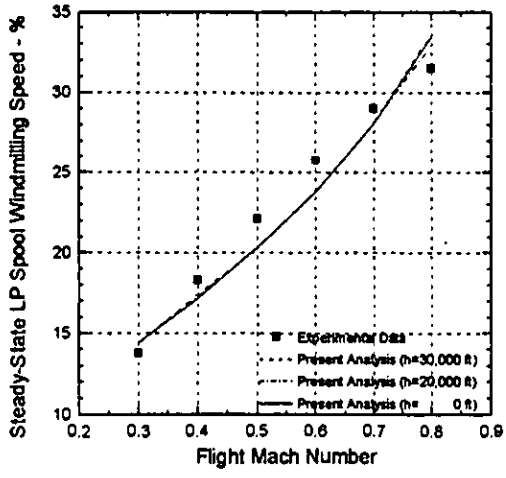

Fig. 7 Steady-state windmilling speed of LP spool
[unit : percent of design speed]

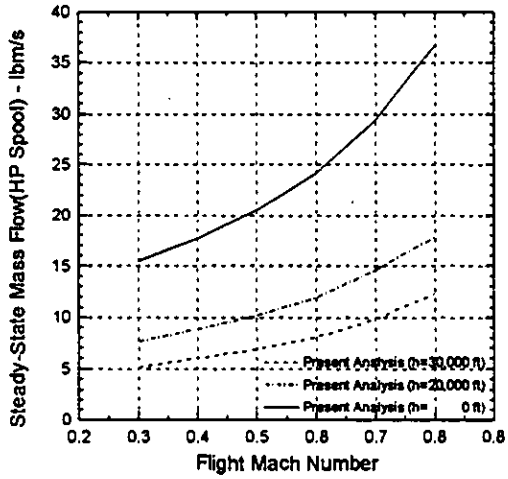

Fig. 8 Steady-state windmilling air flow rate of HP spool

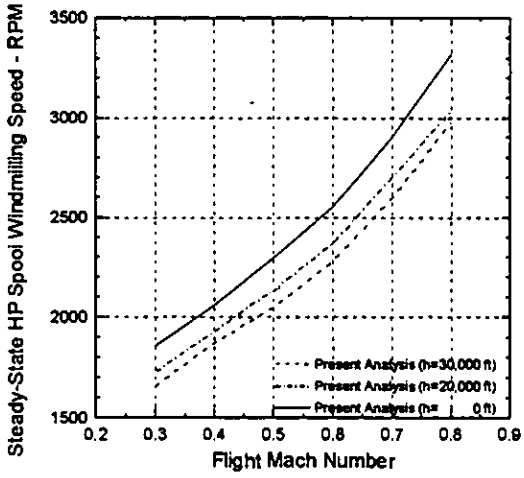

Fig. 9 Steady-state windmilling speed of HP spool